



Published in final edited form as:

*Chem Commun (Camb)*. 2015 May 21; 51(41): 8618–8621. doi:10.1039/c5cc02204e.

## Structural basis for Na<sup>+</sup>-sensitivity in dopamine D2 and D3 receptors†

Mayako Michino<sup>a,b</sup>, R. Benjamin Free<sup>c</sup>, Trevor B. Doyle<sup>c</sup>, David R. Sibley<sup>c</sup>, and Lei Shi<sup>a,b,d</sup>

<sup>a</sup>Department of Physiology and Biophysics, Weill Medical College of Cornell University, New York, NY, USA

<sup>b</sup>Computational Chemistry and Molecular Biophysics Unit, National Institute on Drug Abuse – Intramural Research Program, National Institutes of Health, Baltimore, MD, USA

<sup>c</sup>Molecular Neuropharmacology Section, National Institute of Neurologic Disorders and Stroke, National Institutes of Health, Bethesda, MD, USA

<sup>d</sup>Institute for Computational Biomedicine, Weill Medical College of Cornell University, New York, NY, USA

### Abstract

To understand the structural basis for the Na<sup>+</sup>-sensitivity of ligand binding to dopamine D2-like receptors, using computational analysis in combination with binding assays, we identified interactions critical in propagating the impact of Na<sup>+</sup> on receptor conformations and on the ligand-binding site. Our findings expand the pharmacologically-relevant conformational spectrum of these receptors.

The phenomenon of Na<sup>+</sup>-sensitivity is conserved among many members of class A G-protein coupled receptors, such as the adrenergic,<sup>2</sup> dopaminergic,<sup>3</sup> adenosine,<sup>4</sup> opioid,<sup>5</sup> and neurotensin<sup>6</sup> receptors. The dopamine D2-like receptors, consisting of the D2, D3, and D4 receptors (D2R, D3R, and D4R), are coupled to the G-protein  $\alpha$  subunits (Gi/o) that inhibit adenylyl cyclase.<sup>7</sup> The binding properties of some ligand classes of these receptors are known to be sensitive to sodium ions (Na<sup>+</sup>)<sup>3,8</sup> – a physiologically relevant level of Na<sup>+</sup> (~150 mM) has been shown to decrease the affinity of agonists including the endogenous agonist dopamine, while enhancing the affinity for some antagonists,<sup>3,9</sup> compared to those in the absence of Na<sup>+</sup>. Although this phenomenon of Na<sup>+</sup>-sensitivity has been experimentally known over many years, the structural basis for the allosteric effects of Na<sup>+</sup> on agonist and antagonist binding has not been elucidated.

In D2R, the mutation of Asp80(2.50)<sup>‡</sup> to Ala or Glu was shown to abolish Na<sup>+</sup>-sensitivity,<sup>8</sup> and it was proposed that the residues near Asp80(2.50) form a square pyramidal Na<sup>+</sup> binding site.<sup>10</sup> In recent years, several ultra-high-resolution crystal structures of class A G-protein

<sup>†</sup>Electronic supplementary information (ESI) available: Experimental and computational details, supplemental table and figures. See DOI: 10.1039/c5cc02204e

Correspondence to: Lei Shi.

<sup>‡</sup>The number in parenthesis indicates the Ballesteros and Weinstein index of the residue.<sup>21</sup>

coupled receptors have revealed that the Na<sup>+</sup>-binding site indeed involves the residue Asp(2.50) (reviewed in Katritch *et al.*<sup>11</sup>). Both the 1.8 Å-resolution adenosine A<sub>2A</sub> receptor structure and the 2.1 Å-resolution β<sub>1</sub> adrenergic receptor (β<sub>1</sub>AR) structure show that a Na<sup>+</sup> ion is coordinated by side chain oxygen atoms of Asp(2.50), Ser(3.39), and three water molecules in the middle of a water-filled channel within the transmembrane (TM) domain.<sup>12</sup> The allosteric effects of Na<sup>+</sup> on ligand binding in D2R have previously been studied by computational simulations.<sup>13</sup> Based on the structures of bovine rhodopsin and β<sub>2</sub>AR, Ericksen *et al.* modeled the Na<sup>+</sup>-induced conformations of D2R using normal mode analysis to rationalize the enhanced binding of substituted benzamides and 1,4-disubstituted piperidines/piperazines (1,4-DAPs).<sup>13a</sup> Based on the structure of β<sub>2</sub>AR, Selent *et al.* modeled the allosteric effects of Na<sup>+</sup> in the *apo* state of D2R using microsecond scale all-atom molecular dynamics (MD) simulations and showed that Na<sup>+</sup> enters the receptor from the extracellular side, binds at Asp(2.50), and locks the rotamer toggle switch Trp(6.48) to the inactive state.<sup>13b</sup> Recently, Filizola and colleagues carried out MD simulations in three subtypes of opioid receptors, and revealed important dynamic nature of Na<sup>+</sup> binding.<sup>14</sup>

To better understand the structural basis of the effect of Na<sup>+</sup> on ligand binding affinity in D2R and D3R, in combination with experimental binding assays, we carried out molecular modeling and simulation analysis of the receptors in complex with ligands whose binding are either sensitive or insensitive to Na<sup>+</sup>.

We first investigated the ability of physiological concentrations of Na<sup>+</sup> to modulate the binding of these antagonist ligands (Fig. S1, ESI<sup>†</sup>) to the D2R and D3R. The affinities of the two substituted benzamides, eticlopride and sulpiride, for the D2R are increased (~3-fold for eticlopride and ~23-fold for sulpiride) in the presence of Na<sup>+</sup> (Fig. 1A and B). This effect of Na<sup>+</sup> on sulpiride binding to the D2R is similar to that previously observed.<sup>3,8</sup> In contrast, the presence or absence of Na<sup>+</sup> does not affect the affinity of the butyrophenones, spiperone (Fig. 1C) or methylspiperone (data not shown), for the D2R. Interestingly, we found that the affinity of the tricyclic antipsychotic, zotepine, for the D2R is decreased by ~7-fold in the presence of Na<sup>+</sup> (Fig. 1D). Similar results were observed with the D3R in that the binding of spiperone was not affected by Na<sup>+</sup>, whereas the binding of sulpiride and eticlopride were increased, and the binding of zotepine was decreased by Na<sup>+</sup> (Fig. S2, ESI<sup>†</sup>). These results illustrate how the Na<sup>+</sup> bound state of the D2R and D3R can differentially affect the binding of different ligands to the receptors.

To computationally investigate atomistic details of the Na<sup>+</sup> effect on the ligand binding modes, these ligands were docked to equilibrated D2R and D3R models based on the D3R crystal structure.<sup>1,15</sup> The initial ligand poses were selected from top-scoring poses, taking into account of the implications from available mutagenesis experimental data (see ESI<sup>†</sup>).

We then performed extensive MD simulations of the resulting receptor–ligand complexes either in the presence or absence of Na<sup>+</sup> bound in the Na<sup>+</sup>-binding site (Table S1, ESI<sup>†</sup>). Throughout the simulations, similar to that observed in the crystal structures, the bound Na<sup>+</sup>

---

<sup>†</sup>Electronic supplementary information (ESI) available: Experimental and computational details, supplemental table and figures. See DOI: 10.1039/c5cc02204e

is stably coordinated by the side chain oxygen atoms of Asp(2.50), Ser(3.39), and three water molecules (Fig. S3, ESI<sup>†</sup>). Other residues including Leu(2.46), Ala(2.49), Met(3.35), Asn(7.45), and Ser(7.46) are within 5 Å and contribute to forming the interaction network that support the Na<sup>+</sup> binding and propagate its impact (Fig. S3, ESI<sup>†</sup>).

The salt bridge interactions between the protonated amines of sulpiride and eticlopride with Asp(3.32) are maintained in both Na<sup>+</sup>-bound and -unbound conditions in D2R and D3R. However, in the absence of Na<sup>+</sup>, the ethyl-pyrrolidine moieties shift down in the OBS (Fig. 2B and C), resulting in altered interactions between the sulfonamide N and the side chains of Ser(5.42) and Ser(5.43) in sulpiride, and the benzamide moiety tilting away from the vertical orientation in eticlopride. On the other hand, the binding mode of spiperone in D3R remains largely the same whether in the presence or absence of Na<sup>+</sup> (Fig. 2D). In both conditions, the phenyl-substituted spiro moiety of spiperone makes more extensive interactions with TM2, TM3 and TM7 compared to sulpiride or eticlopride, which may be masking the effect of Na<sup>+</sup> on the ligand binding mode. Interestingly, unlike for sulpiride, eticlopride, and spiperone, the binding mode for zotepine in D2R forms the salt bridge interaction with Asp114(3.32) only in the presence of Na<sup>+</sup>. In the absence of Na<sup>+</sup>, this interaction is lost, and the protonated amine and the ethoxy O atom form an optimal intramolecular interaction, which may contribute to higher binding affinity of zotepine in the Na<sup>+</sup>-unbound condition (Fig. 2E). To further evaluate the role of this intramolecular interaction of zotepine, we characterized the conformational energetics of zotepine and its analog in which the O6 atom is replaced by a C atom, and found that the intramolecular interaction would stabilize zotepine in its lowest-energy conformers, whereas the analog prefers an extended conformation (Fig. S4, ESI<sup>†</sup>). Furthermore, MD simulations of D2R in complex with the zotepine-analog showed that the salt bridge interaction with Asp114(3.32) is maintained in the Na<sup>+</sup>-unbound condition (Fig. S5, ESI<sup>†</sup>). Thus, the binding modes of Na<sup>+</sup>-sensitive ligands, sulpiride, eticlopride, and zotepine, are dependent on the presence of Na<sup>+</sup>, while that of the Na<sup>+</sup>-insensitive ligand, spiperone, is unaffected by the absence of Na<sup>+</sup> (Fig. 2B–E).

To correlate the differential binding modes of Na<sup>+</sup>-(in)sensitive ligands with experimentally observed binding affinities, we calculated the MM/GBSA receptor–ligand binding energy for the frames of the equilibrated portions of the MD trajectories. In agreement with the experimental findings, for sulpiride and eticlopride, the binding energy values were lower (higher affinity) for the ligand poses in the Na<sup>+</sup>-bound condition than the -unbound condition (Fig. 3A and B); while for spiperone, the binding energy values with and without Na<sup>+</sup> were comparable (Fig. 3C). For zotepine, the binding energy values are lower in the Na<sup>+</sup>-unbound condition, consistent with the experimentally observed slightly enhanced affinity in the absence of Na<sup>+</sup> (Fig. 3D).

To characterize the allosteric impact of Na<sup>+</sup> on the receptor conformations that might have contributed to the differential binding modes of Na<sup>+</sup>-sensitive ligands in the presence and absence of Na<sup>+</sup>, we analyzed and compared the changes in the interaction network between the Na<sup>+</sup>-bound vs. -unbound conditions. Our analysis for D3R and D2R in complex with sulpiride showed that the presence of Na<sup>+</sup> strengthens interactions not only in the vicinity of the Na<sup>+</sup>-binding site amongst TMs 2, 3, 6, and 7 (see below), but the impact is also propagated to the extracellular ends of TMs 1, 2, and 7, and to the intracellular ends of TMs

3 and 5 (Fig. 4A). This change in interaction network correlates well with the principal mode of motion calculated by the principal component analysis of trajectories. In the Na<sup>+</sup>-unbound condition, the primary motion can be characterized by an outward movement of the extracellular segments of TMs 1, 2, 7, whereas in the Na<sup>+</sup>-bound condition, the motion is smaller and in the inward direction, consistent with the strengthened interactions in this region in the presence of Na<sup>+</sup> (Fig. 4B). By contrast, similar analysis for the D3R–spiperone complex did not show a marked difference between the Na<sup>+</sup>-bound vs. -unbound trajectories.

Specifically, in the Na<sup>+</sup> binding site, the rotamer state of Ser(3.39) is maintained near  $\chi_1 = -60$  degrees in the Na<sup>+</sup>-bound condition, similarly to that in the D3R structure,<sup>1</sup> while in the Na<sup>+</sup>-unbound condition, the rotamer fluctuates among multiple rotamer states (Fig. S6, ESI<sup>†</sup>). In the ligand binding site, a hydrogen bond interaction between the side chains of Asp(3.32) and Tyr(7.43) located above the Na<sup>+</sup>-binding site is easily broken in the absence of Na<sup>+</sup> – the distance between the carboxylate O of the Asp(3.32) side chain and the hydroxyl O of the Tyr(7.43) side chain is ~3 Å in the Na<sup>+</sup>-bound trajectories, compared to >5 Å in the Na<sup>+</sup>-unbound trajectories in simulations with Na<sup>+</sup>-sensitive ligands, sulpiride, eticlopride, and zotepine (Fig. S7A, ESI<sup>†</sup>). The breaking of this hydrogen bond may contribute to the altered binding mode of these ligands in the Na<sup>+</sup>-unbound condition. Interestingly, our comparative analysis of the eticlopride and sulpiride simulations indicate that eticlopride is more rigid in the binding site, which may facilitate Asp(3.32) to interact with Tyr(7.43) (Fig. S8, ESI<sup>†</sup>). Thus, eticlopride would rely less on the bound-Na<sup>+</sup> to stabilize the Asp(3.32)–Tyr(7.43) interaction, consistent with the lower Na<sup>+</sup> sensitivity of eticlopride than sulpiride (Fig. 1).

In the region adjacent to both the ligand and Na<sup>+</sup>-binding sites, the interactions among TMs 3 and 6, specifically between Cys(3.36) and Phe(6.44), are less frequently formed in the Na<sup>+</sup>-unbound conditions (Fig. S7B, ESI<sup>†</sup>). Interestingly, Phe(6.44) is part of the so-called “P-I-F” motif which reconfigures between the active and inactive states of the  $\beta_2$ AR.<sup>17</sup> The rearrangement observed between TM3 and TM6 from the Na<sup>+</sup>-bound to -unbound condition is in the same direction as that from the inactive to active state (Fig. S7, ESI<sup>†</sup>). At the extracellular ends of TMs 1, 2, and 7, the TM1–TM2 and TM1–TM7 interfaces are each strengthened by two pairwise residue interactions in the Na<sup>+</sup>-bound condition (Fig. 4A).

Although the crystal structure of D3R was not resolved with a bound Na<sup>+</sup>,<sup>1</sup> based on the differing rotamer states of Ser(3.39) in the presence and absence of Na<sup>+</sup>, our analysis strongly supports the presence of Na<sup>+</sup> at Asp(2.50), consistent with a retrospective analysis of this medium resolution structure that showed electron densities compatible with Na<sup>+</sup> in close proximity to Asp(2.50).<sup>11</sup> Our findings also indicate that the presence of Na<sup>+</sup> has an allosteric impact on the ligand binding site, consequently altering the ligand binding mode and modulating the binding affinity of Na<sup>+</sup>-sensitive ligands. In particular, Na<sup>+</sup> binding is associated with a critical interaction between the side chains of Asp(3.32) and Tyr(7.43) located in between the Na<sup>+</sup>-binding site and the ligand binding site. In the Na<sup>+</sup>-unbound condition, the less than optimal binding modes of Na<sup>+</sup>-sensitive ligands, eticlopride and sulpiride, are correlated with the weakening or breaking of this hydrogen bond interaction,

whereas the binding modes of the Na<sup>+</sup>-insensitive ligand, spiperone, appear to mask the impact of the bound Na<sup>+</sup>.

Intriguingly, the critical role of Asp(3.32)–Tyr(7.43) interaction we identified in this study for the binding of Na<sup>+</sup>-sensitive ligands is consistent with the results from a previous study,<sup>19</sup> in which the mutation of Tyr(7.43) to Cys decreased the binding of sulpiride 185 fold, whereas it reduced the binding of Na<sup>+</sup>-insensitive methyl-spiperone only 3 fold. In addition to the effect on ligand binding affinity, Na<sup>+</sup>-binding has also been implicated in modulating signaling efficacy (see ESI<sup>†</sup> for further discussion).

In this communication, the results of our comparative analysis of the MD simulations in the presence or absence of bound Na<sup>+</sup> reveal an allosteric interaction network from the Na<sup>+</sup>-binding site to both the extracellular and intracellular sides of the TM domain and underlie the Na<sup>+</sup>-sensitivity of ligands. Thus, we establish the allosteric mechanism by which ligand binding affinity is modulated in the presence of bound Na<sup>+</sup> at Asp(2.50). The distinct conformations of the receptor bound to Na<sup>+</sup>-sensitive vs. Na<sup>+</sup>-insensitive antagonists studied herein represent sub-states of the inactive state. These conformations will aid in providing a pharmacologically relevant ensemble of receptor conformations in the structure-based virtual high-throughput screening for novel ligand discovery.<sup>20</sup>

## Supplementary Material

Refer to Web version on PubMed Central for supplementary material.

## Notes and references

1. Chien EY, Liu W, Zhao Q, Katritch V, Han GW, Hanson MA, Shi L, Newman AH, Javitch JA, Cherezov V, Stevens RC. *Science*. 2010; 330:1091. [PubMed: 21097933]
2. Limbird LE, Speck JL, Smith SK. *Mol Pharmacol*. 1982; 21:609. [PubMed: 6125876]
3. Neve KA. *Mol Pharmacol*. 1991; 39:570. [PubMed: 2017157]
4. Gao ZG, Kim SK, Gross AS, Chen A, Blaustein JB, Jacobson KA. *Mol Pharmacol*. 2003; 63:1021. [PubMed: 12695530]
5. Pert CB, Pasternak G, Snyder SH. *Science*. 1973; 182:1359. [PubMed: 4128222]
6. Martin S, Botto JM, Vincent JP, Mazella J. *Mol Pharmacol*. 1999; 55:210. [PubMed: 9927610]
7. Fredriksson R, Lagerstrom MC, Lundin LG, Schiöth HB. *Mol Pharmacol*. 2003; 63:1256. [PubMed: 12761335]
8. Neve KA, Cox BA, Henningsen RA, Spanoyannis A, Neve RL. *Mol Pharmacol*. 1991; 39:733. [PubMed: 1828858]
9. (a) Neve KA, Henningsen RA, Kinzie JM, De Paulis T, Schmidt DE, Kessler RM, Janowsky A. *J Pharmacol Exp Ther*. 1990; 252:1108. [PubMed: 2138666] (b) Schetz JA, Sibley DR. *J Pharmacol Exp Ther*. 2001; 296:359. [PubMed: 11160618]
10. Neve KA, Cumbay MG, Thompson KR, Yang R, Buck DC, Watts VJ, DuRand CJ, Teeter MM. *Mol Pharmacol*. 2001; 60:373. [PubMed: 11455025]
11. Katritch V, Fenalti G, Abola EE, Roth BL, Cherezov V, Stevens RC. *Trends Biochem Sci*. 2014; 39:233. [PubMed: 24767681]
12. (a) Liu W, Chun E, Thompson AA, Chubukov P, Xu F, Katritch V, Han GW, Roth CB, Heitman LH, Ijzerman AP, Cherezov V, Stevens RC. *Science*. 2012; 337:232. [PubMed: 22798613] (b) Miller-Gallacher JL, Nehme R, Warne T, Edwards PC, Schertler GF, Leslie AG, Tate CG. *PLoS One*. 2014; 9:e92727. [PubMed: 24663151]

13. (a) Ericksen SS, Cummings DF, Weinstein H, Schetz JA. *J Pharmacol Exp Ther.* 2009; 328:40. [PubMed: 18849360] (b) Selent J, Sanz F, Pastor M, De Fabritiis G. *PLoS Comput Biol.* 2010; 6:e1000884. [PubMed: 20711351]
14. Shang Y, LeRouzic V, Schneider S, Bisignano P, Pasternak GW, Filizola M. *Biochemistry.* 2014; 53:5140. [PubMed: 25073009]
15. Michino M, Donthamsetti P, Beuming T, Banala A, Duan L, Roux T, Han Y, Trinquet E, Newman AH, Javitch JA, Shi L. *Mol Pharmacol.* 2013; 84:854. [PubMed: 24061855]
16. Cheng Y, Prusoff WH. *Biochem Pharmacol.* 1973; 22:3099. [PubMed: 4202581]
17. Rasmussen SG, Choi HJ, Fung JJ, Pardon E, Casarosa P, Chae PS, Devree BT, Rosenbaum DM, Thian FS, Kobilka TS, Schnapp A, Konetzki I, Sunahara RK, Gellman SH, Pautsch A, Steyaert J, Weis WI, Kobilka BK. *Nature.* 2011; 469:175. [PubMed: 21228869]
18. Michino M, Beuming T, Donthamsetti P, Newman AH, Javitch JA, Shi L. *Pharmacol Rev.* 2015; 67:198. [PubMed: 25527701]
19. Fu D, Ballesteros JA, Weinstein H, Chen J, Javitch JA. *Biochemistry.* 1996; 35:11278. [PubMed: 8784181]
20. Osguthorpe DJ, Sherman W, Hagler AT. *J Phys Chem B.* 2012; 116:6952. [PubMed: 22424156]
21. Ballesteros JA, Weinstein H. *Methods Neurosci.* 1995; 25:366.

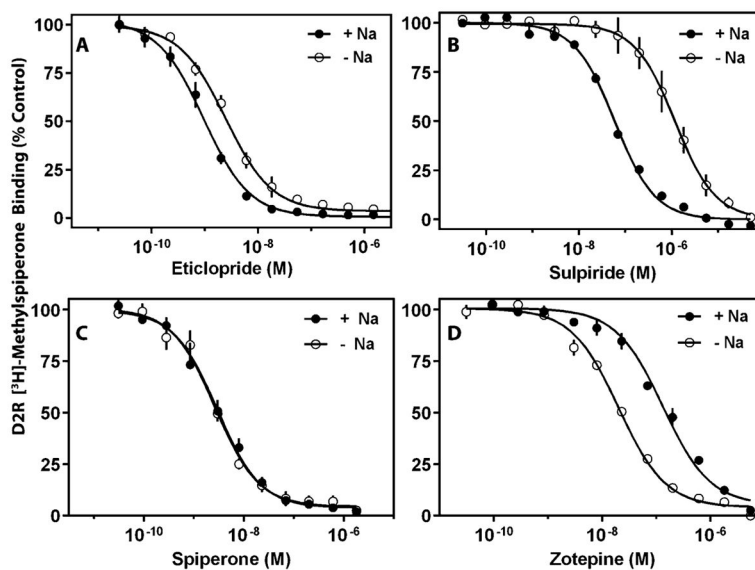


**Fig. 1.**

Experimental binding affinity curves of D2R with and without  $\text{Na}^+$  for eticlopride (A), sulpiride (B), spiperone (C), and zotepine (D). Radioligand binding assays with D2R containing membranes were performed as described in the Methods section. Membranes were incubated with 0.5 nM [ $^3\text{H}$ ]-methylspiperone and the indicated concentrations of competing ligand in the absence or presence of 144 mM  $\text{Na}^+$ . The data are expressed as a percentage of the control [ $^3\text{H}$ ]-methylspiperone binding observed in the absence of a competing ligand. The curves represent an average of three independent experiments.  $K_i$  values were calculated from the  $\text{IC}_{50}$  values using the Cheng–Prusoff equation<sup>16</sup> and are as follows: eticlopride:  $0.67 \pm 0.11$  nM ( $-\text{Na}^+$ ),  $0.27 \pm 0.03$  nM ( $+\text{Na}^+$ ); sulpiride:  $379 \pm 141$  nM ( $-\text{Na}^+$ ),  $16.7 \pm 1.6$  nM ( $+\text{Na}^+$ ); spiperone:  $0.77 \pm 0.12$  nM ( $-\text{Na}^+$ ),  $0.83 \pm 0.26$  nM ( $+\text{Na}^+$ ); zotepine:  $5.8 \pm 0.5$  nM ( $-\text{Na}^+$ ),  $38.4 \pm 5$  nM ( $+\text{Na}^+$ ).



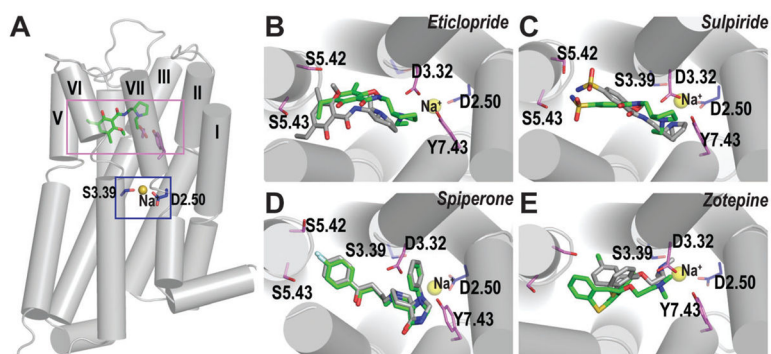


**Fig. 2.**

Ligand binding mode of  $\text{Na}^+$ -sensitive and -insensitive ligands. (A) The relative locations of the  $\text{Na}^+$ -binding site (blue rectangle) and the ligand binding site (violet rectangle) are shown in the D3R-eticlopride structure.<sup>1</sup> The  $\text{Na}^+$  modeled into the structure is coordinated by the side chain oxygen atoms of Asp(2.50) and Ser(3.39), shown in blue sticks. The  $\text{Na}^+$  is shown as yellow spheres. The ligand binding modes of the  $\text{Na}^+$ -sensitive ligands, eticlopride (B), sulpiride (C) and zotepine (E), differ in the  $\text{Na}^+$ -bound (green) vs.  $\text{Na}^+$ -unbound (gray) conditions, while those of  $\text{Na}^+$ -insensitive ligand, spiperone (D), are similar in both conditions.



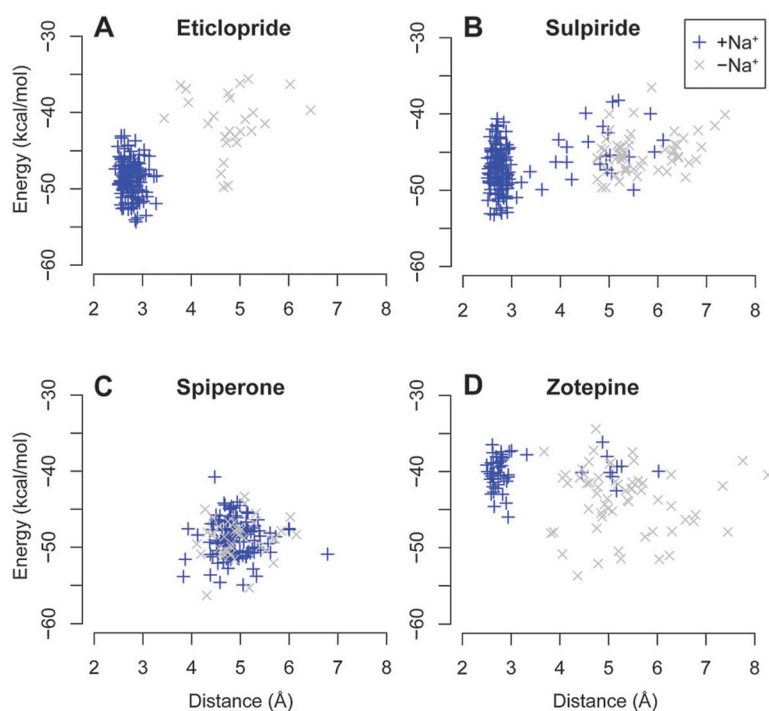


**Fig. 3.** Ligand binding energy and receptor conformation. The MM/GBSA ligand binding energies are plotted against the Asp(3.32)–Tyr(7.43) distances in the eticlopride (A), sulpiride (B), spiperone (C), and zotepine (D) complexes. The Na<sup>+</sup>-bound condition is in blue, and the -unbound condition is in gray. The binding energy and distance values are calculated for the frames at 6 ns-interval in the equilibrated portions of the MD trajectories.

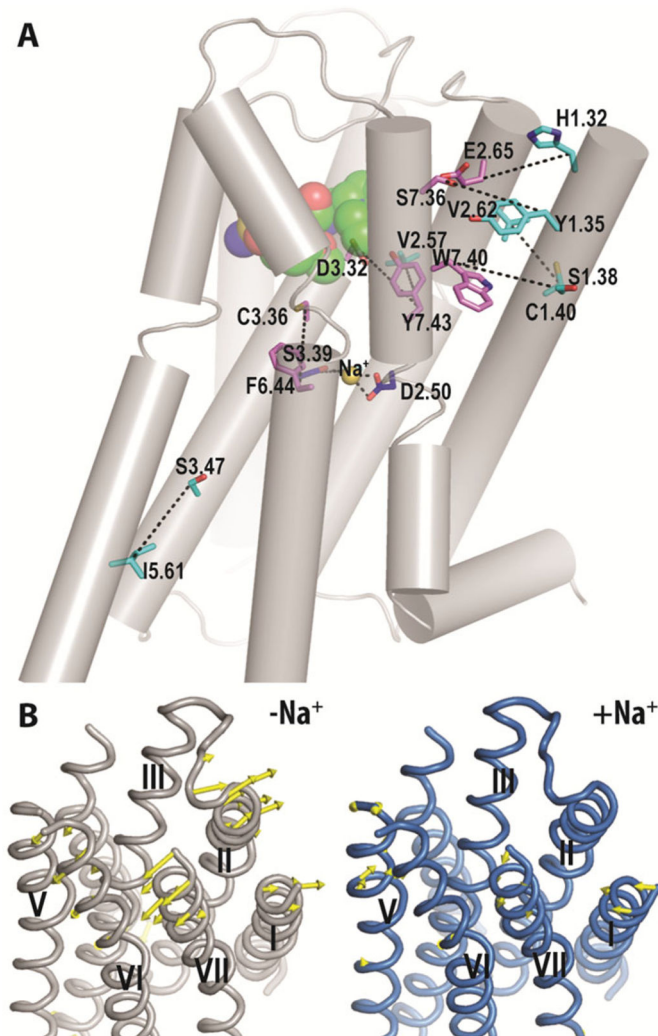


**Fig. 4.** Allosteric impact of  $\text{Na}^+$  on the TM domain. (A) The  $\text{Na}^+$ -modulated interaction network commonly found in D3R–sulpiride and D2R–sulpiride complexes is shown in black dotted lines drawn between residue pairs with significantly different interaction frequencies in the  $\text{Na}^+$ -bound condition compared to the  $\text{Na}^+$ -unbound condition. The residues shown are for D3R. The  $\text{Na}^+$ -coordinating residues are in blue sticks; the residues that may involve in ligand binding<sup>18</sup> are in violet sticks; the remaining residues in the network are in cyan sticks. Sulpiride is in green spheres. (B) The principal mode of motion calculated by the principal component analysis is shown in yellow arrows for the D3R-sulpiride complex in the  $\text{Na}^+$ -bound (blue) and  $\text{Na}^+$ -unbound (gray) conditions.